

This is an Open Access document downloaded from ORCA, Cardiff University's institutional repository: <https://orca.cardiff.ac.uk/id/eprint/102076/>

This is the author's version of a work that was submitted to / accepted for publication.

Citation for final published version:

Giles, Anthony P. , Kay, P. J., Mouzakitidis, Kyriakos, Bowen, Philip John and Crayford, Andrew Philip 2017. On flammability hazards from pressurised high-flashpoint liquid releases. *Journal of Loss Prevention in the Process Industries* 46 , pp. 185-194. 10.1016/j.jlp.2017.01.024

Publishers page: <http://dx.doi.org/10.1016/j.jlp.2017.01.024>

Please note:

Changes made as a result of publishing processes such as copy-editing, formatting and page numbers may not be reflected in this version. For the definitive version of this publication, please refer to the published source. You are advised to consult the publisher's version if you wish to cite this paper.

This version is being made available in accordance with publisher policies. See <http://orca.cf.ac.uk/policies.html> for usage policies. Copyright and moral rights for publications made available in ORCA are retained by the copyright holders.



On Flammability Hazards from Pressurised High-Flashpoint Liquid Releases

Giles A.P.*^a, Kay P.J.^b, Mouzakitis K.^a, Bowen P.J.^a, Crayford A.P.^a

^aCardiff School of Engineering, Cardiff University, Wales, UK

^bDepartment of Engineering Design and Mathematics, University of the West of England, UK.

*Corresponding author: Email GilesAP1@cardiff.ac.uk Tel +44(0) 29 2087 5931

Abstract

Hazardous area classification is well established for dust and vapours, however this is not the case for high flashpoint liquid fuels. This study highlights the limitations of current guidance in relation to flammable mists, through demonstration of flammability of a representative high flashpoint fuel for releases in the range of representative industrial operating pressure, complemented by a phenomenological analysis and semi-quantification of the results observed.

Flammability results are presented from low-pressure practical releases (< 20barg) of a representative fuel (gas-oil with flashpoint > 61 °C), through a plain orifice, at temperatures well below its flashpoint. Based on a proposed two-phase flow-regime diagram, a semi-quantitative analysis of the results observed is offered via a simple 1-D phenomenological model, accommodating jet breakup length, spray quality, air entrainment and droplet dynamics.

The complex scenario of liquid releases impinging onto an unheated flat surface is also considered. An impingement model is utilised to show the relative increase in volume of fine secondary spray induced post-impingement relative to the unobstructed case, resulting in a significant volume of flammable mist. This is demonstrated experimentally by showing flammability of a 5 barg release post impingement whereas the unobstructed 10 barg case would not ignite.

Key Words: Area classification; Explosion hazards; DSEAR; Mist flammability

1. Introduction

The European ATEX directives (99/92/EC and 94/9/EC), published by the European Commission (1999, 1994) are implemented in the UK by the HSE (2002, 1996) under the Dangerous Substances and Explosive Atmospheres Regulations (DSEAR) and the Equipment and Protective Systems Intended for Use in Potentially Explosive Atmospheres Regulations (EPS); requiring employers to classify areas into zones where explosion hazards may occur. Suitably designed equipment must be used within these zones to limit the potential of an accidental ignition. Although hazardous area classification for gases and dust explosion hazards is well established (Eckhoff, 2006), the same cannot be said for mist explosion hazards - particularly for High Flashpoint liquids Fuels (HFF) - as first highlighted by Bowen and Shirvill(1994).

Little progress has been made since this first notification, though the potential exacerbation of the hazard due to jet/spray impingement has again been highlighted by Bowen (2011), and a recent literature review by Santon (2009) of a range of incidents has shown that mist explosions are more common and the consequences more severe than previously anticipated. Santon (2009) identified 37 incidents including 20 explosions, of which nine were collectively responsible for a total of 29 fatalities. This background of a proven explosion hazard without sufficiently rigorous, nor helpful regulation and guidance has provided the motivation of this study.

For flammable gas hazards, the classification of hazardous areas into zones is based on an assessment of the frequency of both the occurrence and duration of the explosive atmosphere, as follows:

- Zone 0: An area in which an explosive gas atmosphere is present continuously or for long periods.
- Zone 1: An area in which an explosive gas atmosphere is likely to occur in normal operation.
- Zone 2: An area in which an explosive gas atmosphere is not likely to occur in normal operation and, if it occurs, will only exist for a short time.

A similar system is applied to dust explosion hazards. Guidance on the classification of areas is provided in IEC 60079-10-1:2015 (BSI, 2015), which applies to gases, vapours and liquids that are handled above their flashpoint

and the potential of a release forming a flammable atmosphere. However, this standard only offers limited quantitative guidance (Annex G) on the potential for liquids handled below their flashpoints generating flammable mists.

The Energy Institute's Model code of safe practice Part 15 (Area classification code for installations handling flammable fluids - EI 15, 2005), does provide some methodology for accounting for mist hazards; but the methodology used for calculating zone extents is not straight forward or suitable for many industrial applications. Adhering to the guidelines and mitigating a mist explosion risk through the use of appropriately rated enclosures and safety systems can be costly. Therefore it is important to understand the parameters that affect the likelihood of an explosive mist atmosphere and can have a quantifiable impact. A Health and Safety Executive report by Gant (2013) comprises of a detailed review of the literature relating to the formation of mists from high flashpoint fluids, the summary of which highlights which fluid properties and release parameters are likely to affect the formation of an explosive mist. A subsequent joint industrial project (Gant et al., 2016) concluded that formation of mists for fuels which are known to fully atomise under practical release conditions can be adequately modelled using computational fluid dynamics codes. However, it was found that the flammable mists that may be formed by a poorly atomised release are more difficult to simulate; and further research is required to understand the formation of such mists.

There are a number of ways a potential flammable mist may be formed. The simplest example to consider is the break-up of a cylindrical liquid jet through a plain orifice, although it is appreciated that realistic accidental releases are likely to be more complicated than this and will include more complicated geometrical orifice characteristics. When a pressurised fluid is forced through an exit orifice, a liquid jet is formed with a velocity proportional to the square root of the pressure differential. As the jet progresses away from the orifice, small instabilities in the jet form and grow until, at some distance downstream, the jet breaks up forming a spray which depending on conditions may form an airborne mist due to minimal gravitational settling. The jet or spray may be obstructed and subsequently impinge on a solid surface, inducing further (secondary) atomisation as shown by Maragkos and Bowen (2002) and potentially creating a finer mist to further exacerbate the situation. Levevre (1989) summarised some of the considerable literature that exists for atomisation and related two-phase phenomena, with previous studies by Kay et al. (2012) showing how such practical releases can still produce > 50 % secondary/primary jet mass-ratio. However, most research and development has been driven by practical applications in sectors such as the automotive or gas turbine industries, which generally consider much smaller orifices and considerably higher release pressures than those likely in accidental release scenarios. Driven primarily by the automotive industry, proposed empirical models for the impingement of droplets and sprays on surfaces have also been developed, examples of which include that of Bai et al (2002) and Mundo et al (1998).

Bane et al (2011) and Shepherd et al (1999) demonstrated that care should be taken when considering 'flammable atmospheres' to differentiate between the ignition characteristics of a droplet spray/mist and the flammability of the fuel/air system. Clearly ignition is a prerequisite for successful flame propagation of fuel droplets, and there is associated literature published examining both fundamental combustion characteristics, deriving for example useful practical concepts such as the minimum ignition energies (E_{min}), the rate of flame propagation (as discussed by Ballal and Lefebvre, 1981) and the upper/lower flammability limits (UFL/LFL). It is important to note, however, that optimum two-phase characteristics for successful ignition do not necessarily correspond to those for optimal fuel-mist flammability. An example of this was shown by Hayashi et al (1981) who established that the MIE generally correspond to < 30 μm droplet mists, dominated by evaporation timescales, whereas the lower flammability limit (LFL) reduces for droplet diameter > 40 μm due to the established inhomogeneous droplet-droplet relay flame propagation mechanism. For this study, this potential source of confusion is allayed, as for all releases considered, those spray/mists that ignited also indeed propagated. Hence, a successful combustion event here means both successful ignition as well as flame propagation i.e. flammability.

The aim of this paper is to develop a better understanding of the extent of this particular hazard, that is to start to put albeit empirical boundaries around the hazardous regimes, as well as to provide an insight into the primary two-phase/combustion processes that give rise to defining the boundaries of this complex hazard, providing guidance of where further work is required.

2. Experimental Techniques and Results

2.1. Experimental Facilities

The experiments were conducted in the Atmospheric Spray Rig (ASR) located at Cardiff University's Gas Turbine Research Centre (GTRC). The ASR is $2.2 \times 1.2 \times 0.7$ m and has the release orifice located at the upstream end and a natural draft extraction at the other. Three spark electrodes were located 0.5, 1.0 and 1.5 m downstream from the orifice respectively; as shown in Fig. 1. Each igniter had a spark gap no greater than 3.8 mm and was connected to a Satronic ZT 870 ignition spark generator. The ignition spark generators are capable of producing a repeatable spark (50 Hz) with a voltage of 16 kV and spark energies of 4 mJ i.e. a relatively low ignition energy, though an order of magnitude greater than the minimum ignition energy (E_{min}) of common fuel vapour. This was selected as a compromise between the unrealistically low minimum ignition energies for common hydrocarbons gases for practical releases; and the broad range of energies which could be encountered in a realistic situation from industrial components (e.g. switchgear, motors). An electrostatic discharge ('brush' discharge) was chosen as a category representing the lower end of realistic industrial ignition sources, and for 'brush' discharges, 4mJ has previously been identified as the theoretical maximum value (Glor M., 1981). The system allows independent firing of each of the igniters, however for the tests presented here the igniters were fired simultaneously.

A nitrogen accumulator was used to pressurise the fuel, enabling a delivery pressure differential of up to 30 bar across the nozzle. The fuel used throughout all the tests was gas-oil (all obtained from a single batch from one supplier) with a quoted flashpoint > 61 °C; this was released at atmospheric temperature, typically 15-20 °C. A pneumatic valve upstream of the orifice controls the timing and duration of the release. The igniters and final valve are controlled remotely. High definition videos of the releases were recorded using a Cannon D60 SLR camera. The release orifice used throughout the experimental program had a diameter of 1 mm and an aspect ratio (L/d) of unity. Whilst appreciating that both these parameters will influence the formation of flammable sprays, neither are varied within this study which aims to highlight the primary processes which need to be taken into consideration. The influence of orifice diameter and L/d should be considered in future studies.

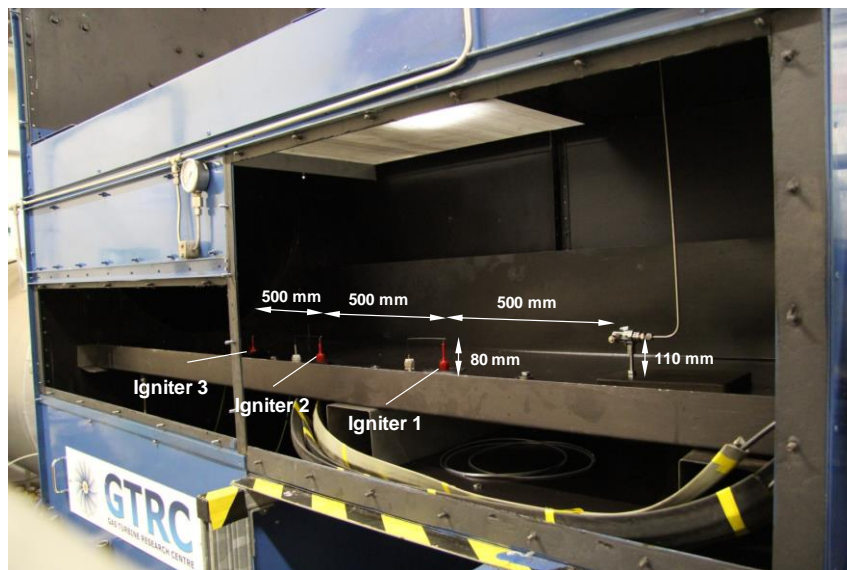


Fig. 1. Overview of rig layout with significant dimensions super imposed.

2.2. Experimental Procedure

The igniters were initiated prior to the fuel being released, and the fuel was sprayed either for a maximum duration of 10 seconds or until ignition was observed. For the impingement tests the set-up remained nominally identical with the only modification being made to the location and orientation of the nozzle. The test chamber was thoroughly cleaned between each test and an exhaust fan utilised to clear any vapour. For the impingement studies the nozzle was located 60 mm from the impingement surface at a perpendicular distance of 100 mm from the first ignitor; fuel was sprayed vertically downwards normal to the flat impingement surface. The surface roughness of the impingement plate was that of a typical cold rolled steel ($R_a \approx 1 \mu\text{m}$), though again the influence of this parameter was not investigated in this study, though previous research by Maragkos and Bowen (2002) has indicated that surface roughness is not a primary influence for these larger scale releases.

The properties of the fuel (gas oil) utilised in this study were provided by the supplier and are presented in Table 1.

Table1. Summary of experimental properties

Parameter	Value
Gas-oil Density [kg/m ³]	837
Gas-oil Viscosity [Pa.s]	4.185 x10 ⁻³
Surface Tension [N/m ²]	0.0264
Air Density [kg/m ³]	1.18
Air Viscosity [Pa.s]	1.846x10 ⁻⁵
Stoichiometric AFR (by mass) [-]	14.9
Orifice Diameter [mm]	1
L/d ₀	1

The experimental results are presented as either a 'positive' or 'negative' event. For a 'negative' event three discrete 10 second releases with no ignition observed at any of the ignitor locations are required. A positive release condition result was defined as an ignition observed at any location, at any time for any of the releases.

2.3. Results

For the free-spray experiments the release pressure was set at an high value initially, and repeat experiments were conducted at decreasing delivery pressures until no ignition was observed during the three repeated releases. Fig. 2 presents two video still images showing pre and post-ignition of the free spray at 25 bar.

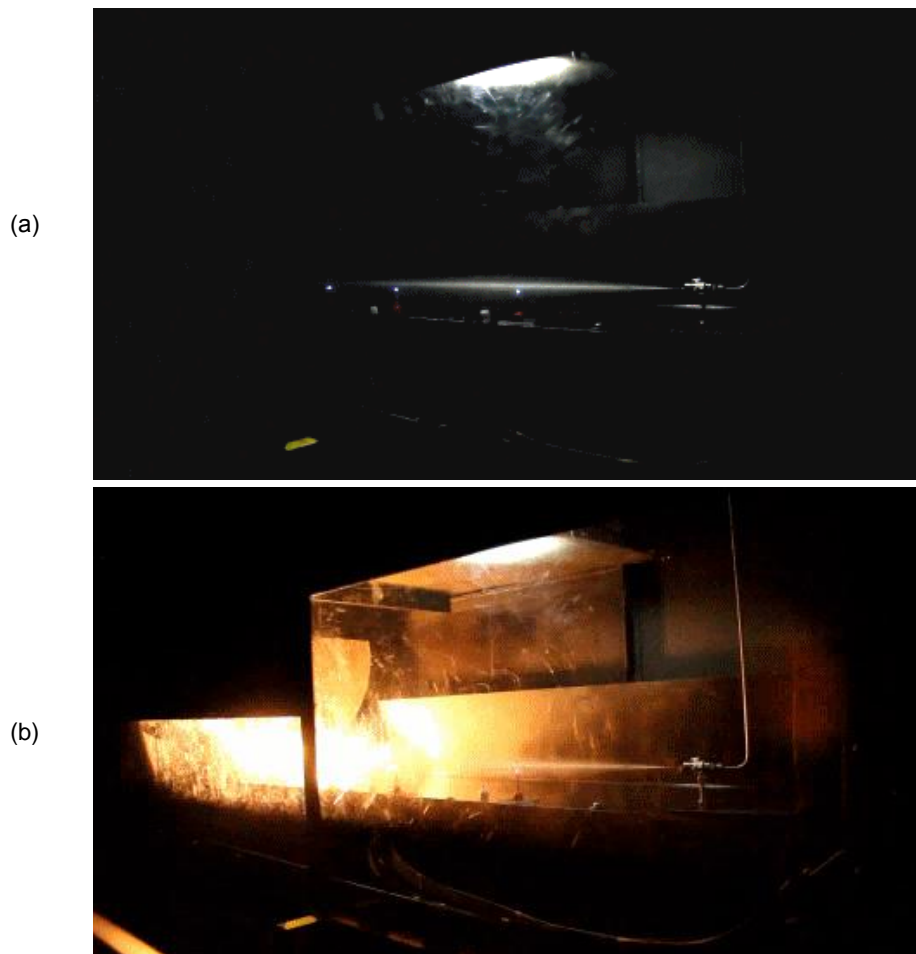


Fig. 2. Video still of ignition of free spray at 25 bar. (a) Pre-ignition and (b) Post-ignition

Once the experimentally derived lower pressure limit for ignition had been identified, the experimental set-up was changed and impinging releases were studied at two release pressures of 10 bar and 5 bar. Table 2 presents a summary of the experimental results.

Table 2. Summary of Experimental results

Test Number	Fuel Pressure [barg]	Set-up	Ignition/Flammability Result (Ignited location{s})
1	25	Free Spray	Positive (1.5 m)
2	20	Free Spray	Positive (1.5 and 1.0 m)
3	15	Free Spray	Positive (1.5 and 1.0 m)
4	10	Free Spray	Negative at all locations
5	10	Impingement	Positive
6	5	Impingement	Positive

3. Analysis and Discussion

Several initial observations can be made from the experimental results presented in Table 2. The first significant observation is that flammable mists were generated for unobstructed pressurised releases at a fuel temperature well below the fuel's flashpoint, highlighting the fact that flashpoint characterisation is insufficient as a measure for assessing the risk of mist flammability. Additionally, the unobstructed sprays proved flammable at relatively low pressures pertinent to, or lower than, conditions used in many industrial applications.

The other significant observation from Table 2 is that impingement of the spray results in a flammable mist at delivery pressures lower than half of that observed for the unobstructed sprays. Consequently, there are many practical applications where fuel is transported at pressures of 10 barg and below, for which any release and likely impingement could pose a mist flammability and potential explosion risk.

This paper will first analyse the unobstructed spray data through the introduction of a simplistic phenomenological modelling approach, followed by analysis of the influence of impingement again through a phenomenological model. The thermo-fluid dynamics associated with the observations will be analysed and discussed, highlighting reasons for the differences in flammability characteristics.

3.1. Unobstructed Spray Analysis

To begin to understand the mechanisms that influence the results observed a simple phenomenological model is presented.

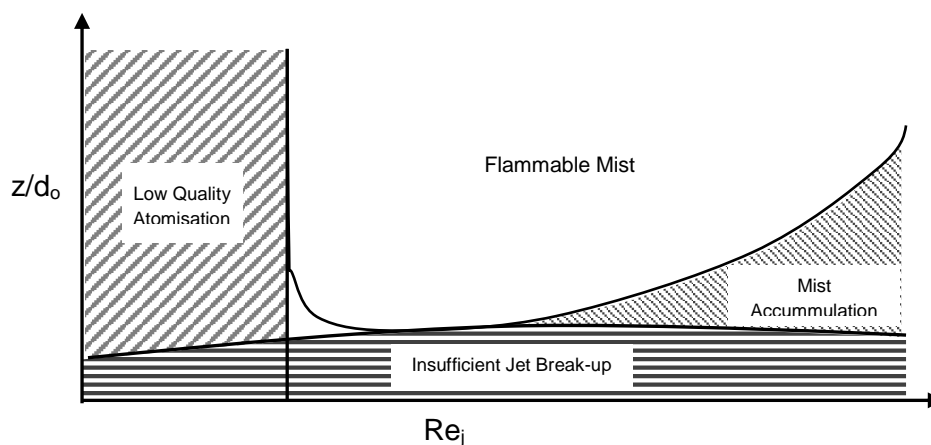


Fig. 3: Simplistic Regime Diagram for determining flammability of pressurized high-flashpoint liquid releases.

The phenomenological flow regime model presented in Fig. 3, is based on well-established phenomena but applied to low pressure releases (≤ 25 barg). The characteristic length used for calculated Re_j is the orifice diameter d_o . The model is split into four different regions:

- **Low Quality Atomisation:** The atomisation pressure is the critical parameter that affects the flow regime of the liquid release and the droplet size distribution for a particular liquid through a specific orifice. For a fixed ignition source there is a critical droplet diameter above which the mist will not ignite. The droplet sizes, and hence their ignitability, are related to the properties of the liquid as well as the initial release conditions.
- **Insufficient Jet Break-up:** Low pressure jet releases breakup over a specific characteristic length and once break-up occurs the air entrainment / liquid dispersion affects the localised air-to-fuel ratio. If an ignition source is within the break-up length, or in a location with minimal dispersion of droplets then ignition will not occur.
- **Flammable Mist:** In the event of a release with sufficient atomisation pressure and where the break-up of the jet has resulted in the mixture of the fuel droplets with sufficient volume of air; if the energy of the ignition source is high enough then the release may ignite. Again dependent upon droplet size and fuel concentration, the flame kernel may subsequently propagate through the combustible two phase mixture.
- **Mist Accumulation (or stratification):** As the pressure of the release and therefore its Reynolds number increases, generally finer mists are generated. However, constituent droplets from finer mists lose their momentum more quickly due to aerodynamic drag, resulting in increased fuel concentration downstream.

3.1.1 Atomisation Pressure

From a comparison of the many spray droplet correlations such as that of Merrington and Richardson (1947), Hiroyasu and Arai (1990), and Faeth (1991). It can be shown that the characteristic droplet size from a liquid release is consistently found to be inversely proportional to the release pressure (typically with an exponent around 0.5-0.6). It is well known that the size distribution in a spray has a significant influence on its combustion characteristics, with finer sprays generally exacerbating combustion hazards due to increased surface area-to-volume ratio.

To compare the sprays at different pressures a representative droplet size distribution developed by Hiroyasu and Arai (1990) is utilised:

$$\text{Mass undersize} = 1 - \exp\left[-\left(\frac{D}{\delta}\right)^\gamma\right] \quad (1)$$

$$\text{where } \delta = 4.12d_o Re_f^{0.12} We_f^{-0.75} \left(\frac{\mu_f}{\mu_a}\right)^{0.54} \left(\frac{\rho_f}{\rho_a}\right)^{0.18} \quad \text{and } \gamma = 2$$

Fig. 4 shows the variation of linear cumulative mass-under-size with log droplet diameter for unobstructed sprays with a release pressure over the experimental range considered here. It is assumed that the boundary conditions are no slip and that there is no further droplet diameter change after the primary atomisation. As the fuel pressure increases, the predicted spray distribution consists of increasingly smaller droplets. The cumulative mass-under-size is of particular importance when considering the probability of successfully igniting a fuel mist, as it is the concentration of ignitable droplets within the vicinity of the ignition source that will determine if a propagating flame is produced.

Moreover, the minimum ignition energy (E_{min}) required to ignite mono-disperse droplet mists has been quantified previously by Ballal and Lefebvre (1978). A validated model was proposed which predicts the E_{min} required to ignite a mono-disperse droplet mist. The E_{min} is related to a number of parameters such as droplet diameter, equivalence ratio (ratio of the actual fuel/air ratio to the stoichiometric fuel/air ratio), gas/liquid properties and evaporation constants :

$$E_{min} = \left(\frac{\frac{1}{6}\pi c_{p,a} \Delta T_{st} D^3}{\rho_a^{1/2}}\right) \cdot \left(\frac{\rho_f}{\phi \ln(1+B_{st})}\right)^{3/2} \quad (2)$$

This is based on the theory of the quenching distance between droplets in a homogeneous quiescent mist established by Ballal and Lefebvre (1978). The minimum ignition energy (E_{min}) is then proposed to be the energy required to raise the temperature a sphere of air, with a diameter equal to the quenching distance, from ambient to the stoichiometric adiabatic flame temperature.

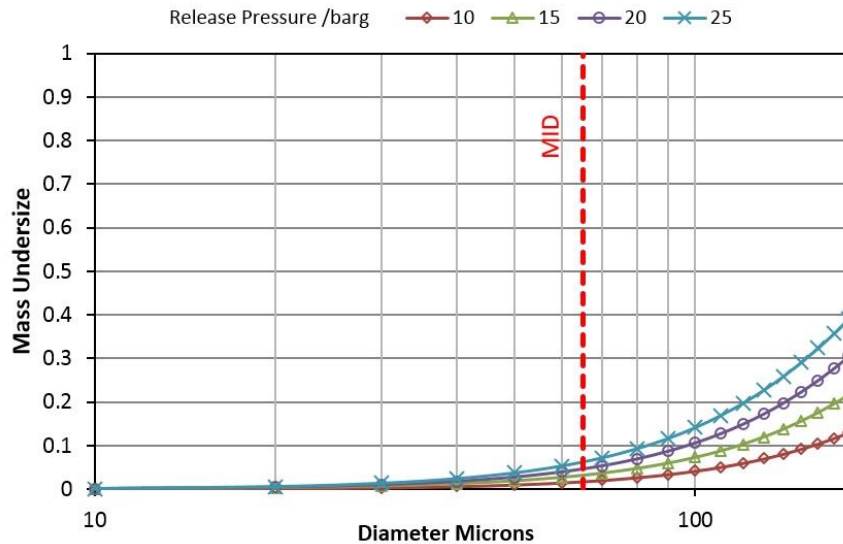


Fig. 4. Variation of mass-under-size for un-obstructed releases of between 10 and 25 barg with MID for stoichiometric conditions super imposed.

The vertical line at 64 microns labelled 'MID' in Fig. 4 represents the largest mono-dispersed droplet size that can be ignited with a E_{min} of 4 mJ for stoichiometric mixture under the ambient conditions of this study. It is noted that for the experimentally unignited 10 barg release, only about 1.75 % of the mass released is predicted to form droplets smaller than the MID whereas the ignitable 15 barg release is estimated to have approximately 3 % of the mass contained in droplets smaller. This suggests that increase in droplet mass undersize with release pressure alone does not fully explain the variation in ignition characteristics with release pressure.

3.1.2 Spray Break-up / Air Entrainment

The experimental results presented in Table 2 show that regardless of fuel pressure, no spray ignited 0.5 m downstream. It is proposed that this is due to the jet break-up length of the spray and insufficient air entrainment. The break-up length of jets from plain orifice atomisers has been studied extensively for automotive applications. Here, two representative correlations of Baron (1949) and Grant and Middleman (1966) are used to predict break-up length.

Over the range of pressure considered here, the two correlations predict the distance to jet break-up to vary between 0.25 and 0.5 m downstream. With the first ignitor being positioned only 0.5 m from the orifice, the predicted break-up lengths indicate why ignition was not observed at this location..

To enable an estimate of downstream air-to-fuel ratio (or equivalence ratio) for each pressure and ignition location, a simplistic one-dimensional approach is developed.

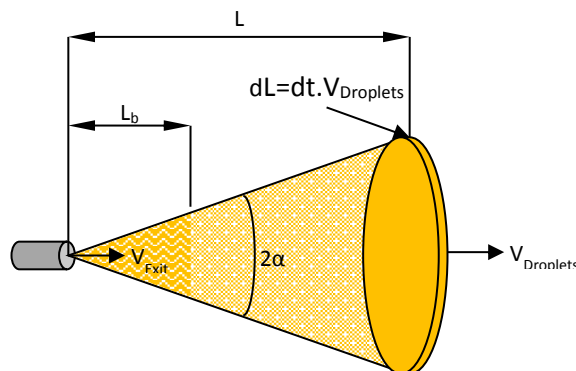


Fig. 5. Schematic of release.

To calculate the mean AFR for a given cross section, a thin disc (dL) at a given distance downstream (L) is considered (see Fig. 5). First, the fuel mass flow rate of the fuel through the disc is determined from Bernoulli's principle, where in a given time (dt) the volume of fuel exiting the release orifice is given by:

$$Volume\ Fuel = dt \cdot V_{Exit} \cdot \pi \cdot (d_o/2)^2 \quad (3)$$

Secondly, the time taken for the fuel to traverse the distance dL is calculated, from which the total volume of air in the disk is calculated:

$$Volume\ Air = dt \cdot V_{Droplets} \cdot \pi \cdot \{[(d_o/2) + L \cdot \tan\alpha]^2 - (d_o/2)^2\} \quad (4)$$

Consequently, it can be shown that the mean AFR (by mass) of a cross section a distance (L) downstream is given by Equation 5.

$$Mean\ AFR = \frac{\rho_a \cdot \{[(d_o/2) + L \cdot \tan\alpha]^2 - (d_o/2)^2\}}{\rho_f \cdot (d_o/2)^2} \cdot \frac{V_{Droplets}}{V_{Exit}} \quad (5)$$

Where α is the spray cone angle, for which many correlations exist such as Arai et al (1984), Hiroyasu and Arai (1985), Chen and Iefebvre (1994), Ruiz and Chigier (1991) and Abramovich (1963). The correlation of Arai et al (1984) agrees most closely with the experimental results where a cone angle $\approx 6^\circ$ was observed for a 20 bar release:

$$\alpha = 0.025 \left(\frac{\rho_a \Delta P d_o^3}{\mu_a^2} \right)^{0.25} \quad (6)$$

In order to calculate the AFR the following assumptions are made. First, it is well established that the majority of the spray's mass is contained in a dense liquid core. To represent this non-uniform distribution, the AFR at different radial positions was calculated using a concentration distribution function based upon measurements made for water releases by Santangelo (2010). The fluid and nozzle type used by Santangelo (2010) was different to that used in this study, however the observed solid cone spray produced when non-dimensionalised is of similar structure, and served the purpose of estimated an AFR at the centreline as opposed to the averaged AFR which would be incorrect. Secondly, the air is considered quiescent and the ratio V_{FUEL}/V_{EXIT} is calculated based on the mean droplet size, as shown by Husted et al (2009). Fig. 6 illustrates the relationship between the value of V_{FUEL}/V_{EXIT} and the distance from the release point as a function of mean droplet size.

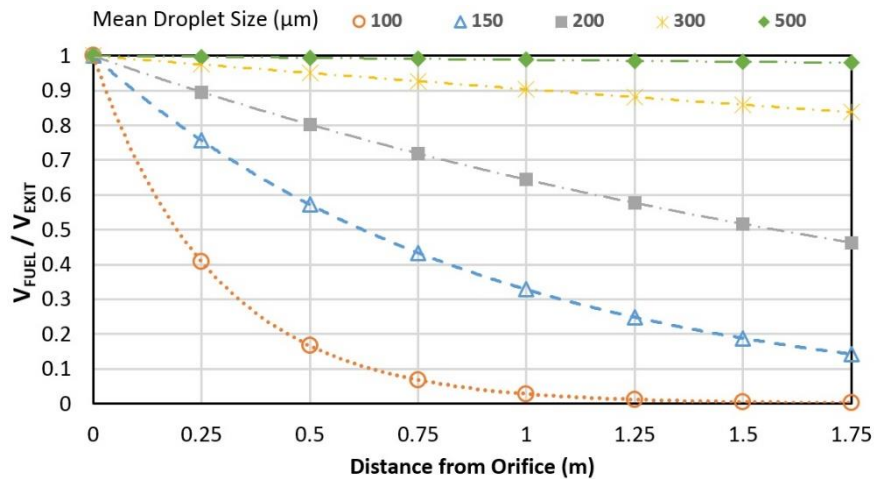


Fig. 6. Relationship between droplet size, distance from orifice and mean velocity

The predicted droplet SMD (droplet diameter having the same volume/surface area ratio as the entire spray) from the representative correlation of Hiroyasu and Arai (1990) is also presented corresponding to the experimental conditions utilised in this study. Fig. 7 shows a graphical representation of the experimental results. The location at which the spray ignited and propagated was determined by examining still images of the videos for each test. A cross (x) represents combustion whereas a circle (●) represents no combustion. Fig. 7 shows sensibly that the fuel-air mixture becomes increasingly fuel-lean as the distance from the orifice increases and the spray propagates radially. It also predicts that the distance at which the fuel-air mixture reaches the stoichiometric concentration is approximately 1.0 m downstream from the orifice. This suggests that the lack of ignition closer to the orifice (ignitor

position 0.5 m downstream) is likely to be due to the mixture being too rich and/or poorly atomised to ignite with the spark characteristics employed. Previous jet break-up predictions from Baron (1949) and Grant and Middleman (1966) are also represented on Fig. 7 by the dash-dot and dotted lines respectively, Baron's predictions in particular appear to correlate well with the ignition failure points 0.5m downstream at all pressures considered.

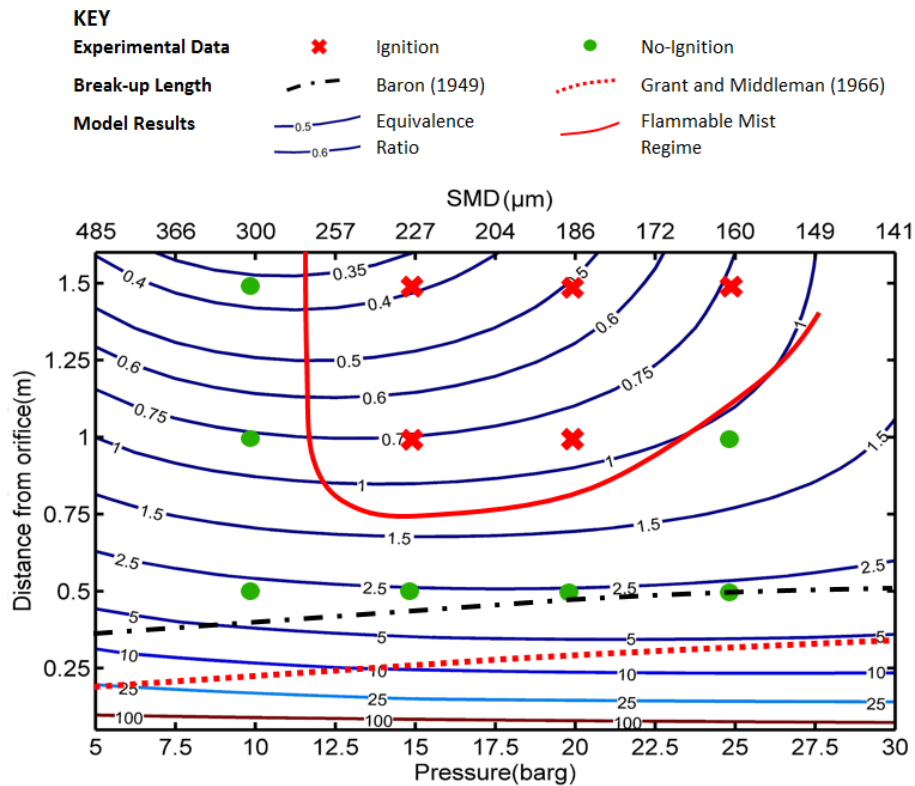


Fig. 7. Gas-oil results with calculated equivalence ratio superimposed.

Fig. 7 also shows the failure of the 10 bar unobstructed releases to ignite at any downstream location with the ignition source adopted, even though the equivalence ratio predictions indicate a flammable atmosphere at the 1.0m downstream ignition location, realised for the 15 bar and 20 bar release cases. Surprisingly, the 25 bar releases at an ignitor position 1.0 m downstream from the orifice did not ignite, even though the equivalence ratio is predicted to be 1.0-1.5.

It is proposed that this non-linear characteristic of spray ignition and flammability as a function of downstream distance, clearly observed in Figs. 7 and 8, may be explained qualitatively through the interaction of several key two-phase processes described earlier and outlined qualitatively in the regime diagram in Fig. 3.

First, the lower release pressure (or generally Re) bound, independent of downstream location, signifies the role of atomisation in the overall process. As discussed earlier, it is well established that ignition probability reduces with reduction in spray quality, and that spray quality reduces with release pressure. This is presented on the upper horizontal axis of Figs. 7 and 8, where the representative pressure-orifice spray correlation – there is some debate concerning the absolute values of spray quality predicted from such correlations, but far less so the influence of pressure - has been utilised to provide an SMD estimate. Hence, as shown the 10 bar release corresponds to a 300 μm SMD prediction for gas-oil, whilst the predicted equivalence ratio at the ignitor locations ranges from circa 0.35-2.5. However, only a very small proportion of the total spray mass will be contained in droplets of a size conducive to ignition and flammability with the source adopted, so that the 'practical' equivalence ratio will be considerably – possibly one to two orders of magnitude – less than that estimated by this simple phenomenological approach. As release pressure (or Re) increases, then the spray quality improves, and so a higher proportion of the spray becomes ignitable and flammable, corresponding to the positive flammability cases presented for the 15 bar and 20 bar releases beyond the influence of the jet break-up length (> 0.5 m).

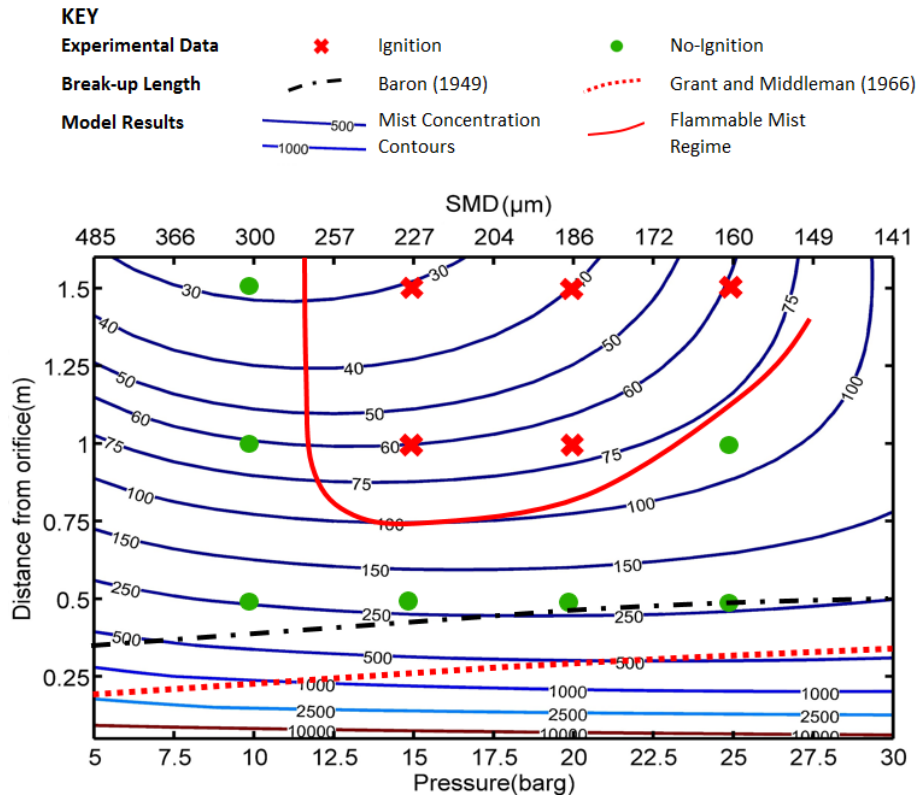


Fig. 8. Gas-oil results with mist concentration (in g/m^3) superimposed.

The ignition failure of the 25 bar release at the 1 m location - beyond the breakup length and generating the best spray quality – is the most subtle and most subjective to interpret : As spray quality improves for the higher-pressure releases, then aerodynamic drag on the droplets increases, and the spray loses its momentum more readily. Put simply, for the same mass flowrate, poorer quality spray will propagate further, spreading its mass over a larger volume than that of a higher quality spray. This results in the sharp non-linear behaviour in the equivalence ratio plots for higher pressures (> 20 bar) observed within Figs. 7 and 8. Whilst this interpretation of the data does not *quantitatively* correspond with the non-ignition of the 20 bar case – the equivalence ratio is predicted to be between 1 and 1.5 – within the spirit and accuracy of the phenomenological approach presented, it is sufficient to indicate that differential droplet-drag and stratification is likely to be a significant contributory factor. In addition, as the release pressure is increased, the mass flux and droplet velocities within the spark vicinity is proportionally increased; reducing the probability of a propagating ignition. Clearly a more accurate model for combining jet-breakup, atomisation and droplet dynamics would further substantiate the proposed model as well as simultaneously take into account the various interdependent processes discussed.

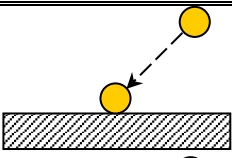
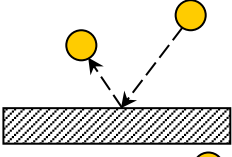
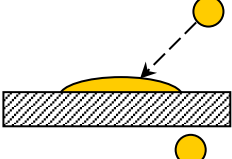
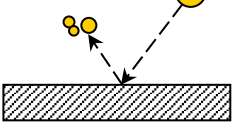
Fig. 8 provides an alternative presentation of the predicted mist concentration (in g/m^3) for the test cases considered, as these figures are often utilised in safety standards. Again the predicted droplet SMD from the Hiroyasu and Arai (1990) correlation and the calculated break-up lengths from Baron (1949) [dashed line] and Grant and Middleman (1966) [dotted line] are also presented.

It is shown that at an ignitor location 1.5 m downstream from the orifice, the predicted mist concentrations for the cases in which ignition occurred (15, 20 and 25 bar) are all in the range of 30 to 65 g/m^3 . It is generally accepted that the LEL for hydrocarbon mists formed by a high velocity spray is considered to be around 50 g/m^3 ; with this value used in several safety standards such as the IACS M67 testing procedure (2007). This suggests that even with mist concentrations below the widely accepted LEL for a hydrocarbon fuel, there is potential risk of ignition and flame propagation if suitable droplet sizes are present. These findings are consistent with those of Zabetakis (1965).

3.2. Impinging Spray Analysis

As presented in Table 2, an impinging flammable spray was observed at lower pressure releases than that for an unobstructed spray. This can be explained by comparing the droplet size distribution of the spray pre and post-impingement. This can be explained by comparing the droplet size distribution of the spray pre and post-impingement. As previously mentioned by Maragkos and Bowen (2002), impingement generally exacerbates the potential hazard due to the potential for re-atomisation of splashing droplets, reducing the mean droplet diameter whilst increasing the number of droplets post-impingement. Considerable effort has been given to understanding the impingement of single and multiple droplet impacts on solid surfaces and developing empirical models that predict post-impingement droplet characteristics. Due to the two-phase thermo-fluid complexity of the impingement process, previous analysis has resorted to the development of phenomenological models, utilising non-dimensionalised correlations. These impingement models are employed in some of the more widely used commercial CFD software with the correlation of Bai *et al* (2002) being one of the most widely used. This model, based on the impacting droplet Weber and Laplace number, first predicts whether the droplet will stick, spread, bounce or splash on the surface. The regime transition criteria are presented in Table 3 with the post impingement droplet characteristics based on separate correlations depending on which regime prevails.

Table 1. Regime transition criteria, Bai *et al* (2002)

Regime	Schematic	Transition Criteria
Stick		$We_d \leq 2630.La^{-0.18}$ (DRY) $We_d \leq 2$ (WET)
Rebound		$2 \leq We_d \leq 20$ (WET)
Spread		$20 \leq We_d \leq 1320.La^{-0.18}$ (WET)
Splash		$We_d > 2630.La^{-0.18}$ (DRY) $We_d > 1320.La^{-0.18}$ (WET)

The Bai *et al* (2002) model is applied to the impinging spray for 10 bar and 5 bar releases, which both resulted in flame propagation (Table 2). The calculated cumulative mass-under-size with log droplet diameter plots of the post-impingement sprays for both release pressures are presented in Fig. 9, along with the calculated unobstructed spray data for the same release pressures; to allow visual comparison between the free and post-impingement sprays. Fig. 9 highlights that for the unobstructed 5 bar release case less than 1 % of the total mass is considered ignitable based on calculated MID criteria. However post-impingement, nearly 70 % of the spray droplets that have “splashed” satisfy the MID criterion. This confirms that the spray quality is a dominant factor concerning ignition and subsequent flame propagation of impinging sprays.

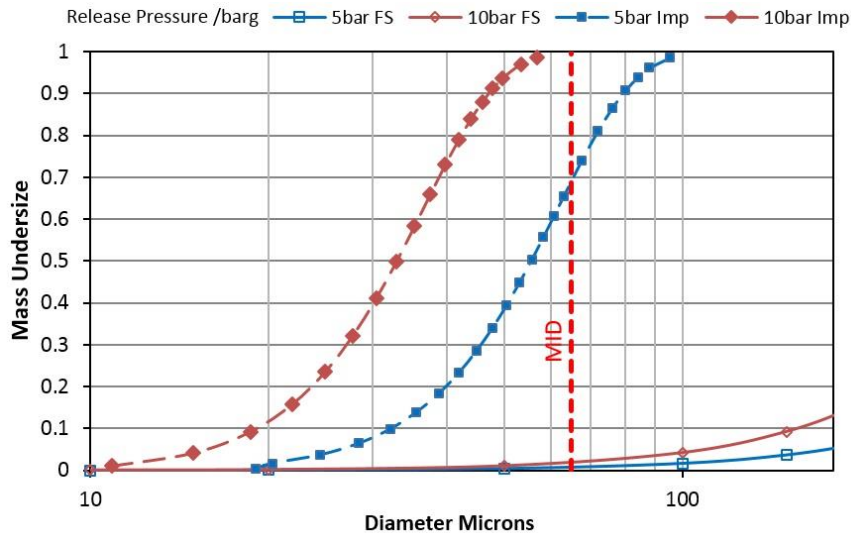


Fig. 9. Variation of mass-undersize for un-obstructed and impinging releases of 5 and 10 barg with MIE for stoichiometric conditions super-imposed.

4. Conclusions

The main conclusions from this study are:

- Under controlled conditions, unobstructed releases of a high flashpoint fuel (gas-oil, flashpoint > 61 °C) through a plain orifice at 15 bar release pressure have been shown to be flammable, at release temperatures some 40 °C below the fuel's flashpoint. This confirms a previous hypothesis of Bowen and Shirvill (1994).
- A two-phase regime diagram has been proposed to describe the combustion region. Whilst this approach qualitatively and semi-quantitatively explains the flammability trends observed in this particular case, the applicability of such a modelling approach more generally cannot be ascertained at this stage, due to limited well-controlled validation data.
- The gas-oil releases that did not provide flammable sprays at 10 bar pressure, were found to become flammable after impingement on a normal surface placed near the release point. The impinging release was also found to be flammable at a reduced pressure (5bar), highlighting the increased risk associated with jet/spray impingement, which is likely in realistic scenarios.
- A phenomenological spray impingement model based upon Weber/Laplace correlations predicts the likely cause of increased flammability for impinging sprays: Whilst the impingement process reduces airborne fuel, this is dominated by a substantial improvement in spray quality, rendering a far higher proportion of the spray within the ignitable and flammable droplet size ranges.
- This paper highlights the lack of published guidance for flammability hazards associated with low-pressure releases of high-flashpoint fuels, Whilst a simplified phenomenological approach is presented here, it is based on results for one high-flashpoint fuel only, with one particular release orifice and a specific low-energy ignition source, This progress needs now to be complemented by more detailed modelling and validation research to enable more robust predictive industrial tools, which are urgently required to provide useful safety guidelines.

Acknowledgements

The authors would like to take this opportunity to thank Mr Steve Morris and Mr Terry Treherne at the Gas Turbine Research Centre, Cardiff University for their assistance during the set-up and delivery of the experimental programme. This research did not receive any specific grant from funding agencies in the public, commercial, or not-for-profit sectors.

Nomenclature

AFR	Air to Fuel Ratio
B_{st}	Spalding Transfer Number
C_p	Specific Heat Capacity [$J.kg^{-1}.K^{-1}$]

D	Droplet Diameter [m]
d_o	Orifice diameter [m]
E_{min}	Minimum Ignition Energy
L	Distance from the nozzle [m]
La	Laplace number = $\sigma \rho_f D \mu_f^{-1}$
LEL	Lower Explosion Limit
MID	Maximum Ignitable Droplet-diameter
ΔP	Pressure differential across the nozzle [Pa]
Re	Reynolds Number = $\rho_f D V \mu_f^{-1}$
SMD	Sauter Mean Diameter [m]
T_{st}	Stoichiometric Flame Temperature [K]
We	Weber Number = $\rho_f D V^2 \sigma^{-1}$
α	Spray cone angle [°]
μ	Viscosity [Pa.s]
ρ	Density [Kg.m ⁻³]
σ	Surface tension [N.m ⁻²]
ϕ	Equivalence Ratio

Subscripts

a	Air
d	Droplet
f	Fuel
j	Jet

References

- Abramovich, G.N., 1963, Theory of turbulent jets. MIT Press, Cambridge, MA.
- Arai, M., Tabata, M., Hiroyasu, H. and Shimizu, M., 1984, *Disintegrating Process and Spray Characterization of Fuel Jet Injected by a Diesel Nozzle*, SAE Paper 840275
- Bai, C.X., Rusche, H. and Gosman, A.D., 2002, Modeling of Gasoline Spray Impingement. *Atomization Spray*, 12, 1-27.
- Ballal, D.R., Lefebvre, A.H., 1978, Ignition and Flame Quenching of Quiescent Fuel Mists. *P Roy Soc Lond*, A364, 277-294.
- Ballal, D.R., Lefebvre, A.H., 1981, Flame propagation in heterogenous mixtures of fuel droplets, fuel vapor and air. *Proc Symp (Int) Comb*, 18, 321-328.
- Bane, S.P.M., Ziegler, J.L., Boettcher, P.A., Coronel, S.A. and Shepherd J.E., 2011, Experimental investigation of spark ignition energy in kerosene, hexane, and hydrogen, *J Loss Prevent Proc*, 26, 290-294
- Baron, T., 1949, Technical Report No. 4, University of Illinois.
- Bowen, P.J., 2011, Combustion Hazards Posed by Hybrid Fuel Systems. Keynote Address at 5th European Combustion Meeting. Cardiff, UK.
- Bowen, P.J., Shirvill, L.C., 1994, Combustion hazards posed by the pressurized atomization of high-flashpoint liquids. *J Loss Prevent Proc*, 7, 233-241.
- BSI, 2015. IEC 60079-10-1:2015 Explosive atmospheres - Part 10-1: Classification of areas - Explosive gas atmospheres, 2015, BSI: London, UK.
- Chen, S.K., Lefebvre, A.H., 1994, Discharge coefficient for plain orifice effervescent atomizers. *Atomization Spray*, 4, 291-301.
- European Commission, 1994, Directive 1994/9/EC, *Off J Eur Communities* L100 37, 1-29.
- European Commission, 1999, Directive 1999/92/EC, *Off J Eur Communities* L23 43, 57-64.
- Eckhoff, R.K., 2006, Differences and similarities of gas and dust explosions: A critical evaluation of the European 'ATEX' directives in relation to dusts. *J Loss Prevent Proc*, 19, 553-560.
- Energy Institute, 2005, Model Code of Safe Practice Part 15: Area Classification Code for Installations Handling Flammable Fluids.
- Faeth, G.M., 1991, *Structure and atomization properties of dense turbulent sprays*. *Proc Symp (Int) Comb*, 23, 1345-1352.
- Gant S.E., 2013, *Generation of flammable mists from high flashpoint fluids: literature review*, Health and Safety Executive, Research Report RR980.
- Gant, S.E., Bettis, R., Coldrick, S. Burrell, G., Santon, R., Fullam, B., Mouzakis, K., Giles, A. and Bowen, P., 2016, *Area classification of flammable mists; summary of joint-industry project findings*, IChemE Hazards 26 Conference, Edinburgh, UK, 24-26 May.

- Glor, M., 1981, *Ignition of gas/air mixtures by discharges between electrostatically charged plastic surfaces and metallic electrodes*, J. Electrostat, 10, 327-332
- Grant, R.P., Middleman, S., 1966, Newtonian Jet Stability. AIChE Journal, 12, 669-678.
- Hayashi S., Ohtani T., Inuma K. and Kumagi S., 1981, Limiting factor of flame propagation in low-volatility fuel clouds. Eighteenth Symposium (International) on Combustion, Comb Inst, 361-367.
- Hiroyasu, H., Arai, M., 1985, Fuel Spray Penetration and Spray Cone Angle in Diesel Engines. Transactions JSAE, 94.
- Hiroyasu H., Arai M., 1990, *Structures of Fuel Sprays in Diesel Engines*, SAE paper 900475.
- HSE, 1996, *Equipment and Protective Systems Intended for Use in Potentially Explosive Atmospheres Regulations 1996* (EPS), (SI 1996/192 HMSO)
- HSE, 2002, *Dangerous Substances and Explosive Atmospheres Regulations 2002*, (SI 2002/2776 HMSO).
- Husted, B.P., Petersson, P., Lund, I. and Holmstedt, G., 2009, Comparison of PIV and PDA droplet velocity measurement techniques on two high-pressure water mist nozzles. Fire Safety J, 44, 1030-1045.
- IACS, 2007, M67 Type testing procedure for crankcase oil mist detection and alarm equipment.
- Kay, P.J., Bowen, P.J., Gold, M.R. and Sapsford, S.M., 2012, Transient fuel spray impingement at atmospheric and elevated ambient conditions. Exp Fluids, 53, 873-890.
- Lefebvre, A.H., 1989, *Atomization and Sprays*. Hemisphere Publishing Corporation.
- Maragkos, A., Bowen, P.J., 2002, Combustion hazards due to impingement of pressurised releases of high flashpoint liquid fuels. Proc Comb Inst, 29, 305-311
- Merrington A.C. and Richardson E.G., 1947, *The break-up of liquid jets*, Proc. Phys. Soc. 59, 1.
- Mundo, C., Sommerfeld, M. and Tropea, C., 1998, On the Modeling of Liquid Sprays Impinging on Surfaces, Atomization Spray, 8, 625-652.
- Ruiz, F., Chigier, N., 1991, Parametric Experiments on Liquid Jet Atomization Spray Angle. Atomization Spray, 1, 23-45.
- Santangelo, P.E., 2010, Characterization of high-pressure water-mist sprays: Experimental analysis of droplet size and dispersion. Exp Therm Fluid Sci, 34, 1353-1366
- Santon, R.C., 2009, Mist fires and explosions - an incident survey, IChemE Hazards XXI Symposium & Workshop. Manchester, UK.
- Shepherd, J.E., Lee, J.J. and Krok, J.C., 1999, Spark ignition energy measurements in Jet A, Graduate Aerospace Laboratories, California Institute of Technology.
- Zabetakis, M.G., 1965, Flammability Characteristics of Combustible Gases and Vapors. Bulletin 627, Bureau of Mines.